Environmental Microbiome

RESEARCH

Open Access

# Microbial generalists as keystone species: constructing core network modules in the anthosphere of twelve diverse wild plant species

Jihoon Kim[1,2†], Yingshun Cui[3†], Kyong-Hee Nam[1], Jun-Woo Lee[1], Jong-Geol Kim[2] and Seong-Jun Chun[1*]

## Abstract

**Background** The anthosphere, also known as the floral microbiome, is a crucial component of the plant reproductive system. Therefore, understanding the anthospheric microbiome is essential to explore the diversity, interactions, and functions of wildflowers that coexist in natural habitats. We aimed to explore microbial interaction mechanisms and key drivers of microbial community structures using 144 flower samples from 12 different wild plant species inhabiting the same natural environment in South Korea.

**Results** The microbial diversity of the anthosphere showed plant dependence, with the highest diversity observed in *Forsythia koreana*, indicating microbial dynamics in relation to plant species. *Caulobacter*, *Sphingomonas*, *Achromobacter*, *Epicoccum*, *Cladosporium*, and *Alternaria* were anthosphere generalists, suggesting that the local plant anthosphere had a similar microbial composition. Ecological network analysis revealed that anthosphere generalists were tightly coupled to each other and constructed core modules in the anthosphere. Functions associated with parasites and pathogens were commonly observed in the anthosphere, particularly in *Capsella bursa-pastoris* and *Brassica juncea*.

**Conclusion** Overall, the anthosphere depends on the plant species and microbial generalists function as keystone species to support and connect the anthospheric microbiome in natural habitats.

**Keywords** Floral microbiome, Functional analysis, Keystone species, Recurrent network analysis, Wildflowers

†Jihoon Kim and Yingshun Cui are the co-first authors and equally contributed to this work.

*Correspondence:
Seong-Jun Chun
sjchun@nie.re.kr
[1]LMO Team, National Institute of Ecology, 1210 Geumgang-ro, Maseo-myeon, Seocheon, Republic of Korea
[2]Department of Biological Science, Wonkwang University, 460 Iksan-daero, Iksan, Republic of Korea
[3]Jeonbuk Institute for Food-Bioindustry, 111-18 Wonjangdong-gil, Deokjin-gu, Jeonju, Republic of Korea

## Background

The plant microbiome is an integral component of the plant holobiont and exerts a significant influence on plant growth, immunity, and evolutionary processes [1, 2]. Among the various parts of the plant microbiome, the anthosphere, also known as the floral microbiome, possesses a distinctive property owing to the relatively short lifespan of flowers compared to that of other plant parts [3]. In addition, the structural complexity of flowers and presence of nectar contribute to the formation of distinct microbial communities in the anthosphere [3, 4]. These dynamic microbial communities interact with various biotic and abiotic factors, such as pollinators, and play crucial roles in plant reproductive ecology and floral evolution [5, 6].

In natural ecosystems, as opposed to cultivated environments, a diverse array of flowers bloom concurrently, attracting a variety of pollinators that visit multiple plant species rather than concentrating on a single species [7]. However, most anthosphere-related studies have focused on individual plant species or have compared only a few species [3, 8–10]. For instance, Qian et al. [9] focused on four wild plant species that grew together in the same environment and observed that the fungal community composition exhibited species-specificity, whereas the bacterial composition did not. Therefore, conducting studies targeting wildflowers that bloom concurrently in the same environment is necessary.

The anthosphere possesses a unique microbial community compared to that of other plant compartments, the origin and dispersal routes of the anthosphere have become a significant research focus [11]. Pollinators attracted by flowers, such as honeybees and butterflies, play crucial roles in the transmission and dispersal of various microbes between anthospheres by carrying their own microbial communities and transferring them from one anthosphere to another [5, 8, 12]. For instance, honeybees can carry phytopathogenic bacteria, such as *Erwinia persicina*, from beehives to flowers and flower to flower, thereby spreading fire blight disease [13]. In addition, the anthosphere is influenced by abiotic factors, such as temperature, wind, and rain, resulting in changes in its composition [11, 14, 15]. Russell and McFrederick [16] demonstrated that temperature can influence nectar properties, thereby affecting microbial community structure.

Recent advances in metagenomic and bioinformatic analyses have helped in uncovering complex interactions within plant holobionts [9, 17, 18]. Because microbial interactions are important for shaping ecological dynamics, network analysis is an effective bioinformatic tool for exploring potential microbial interactions within complex communities [19, 20]. Qian et al. [9] employed network analysis to reveal the co-occurrence patterns and interactions within the anthospheres of four plant species. Consequently, tools such as PICRUSt2, FAPROTAX, and FUNGuild have been developed to translate community structure data into functional data. Therefore, applying advanced metagenomics and bioinformatics analyses to anthosphere research is essential for unraveling complex microbial interactions and understanding their roles in the anthosphere [17].

In this study, we focused on investigating the anthospheres of 12 commonly observed but understudied plant species in South Korea during this season. The aim of this study was to elucidate the microbial generalists and specialists of the anthosphere from 12 different plant species coexisting in the same environment and investigate whether conserved or unique interactions are present via network analysis, thereby identifying the ecological roles of these anthosphere. In addition, we present the first anthospheric study of six different plant species: *Veronica polita*, *Taraxacum mongolicum*, *Forsythia koreana*, *Chelidonium majus* subsp. *asiaticum*, *Prunus* × *yedoensis*, and *Viola mandshurica*.

## Methods

### Obtaining flower samples and compiling plant characteristics

Spring is one of the major periods in temperate climates, characterized by a wide variety of blooming flowers and the simultaneous activity of many pollinators. Anthosphere sampling was conducted on April 8, 2022, in Gurye, South Korea (35.19°N, 127.47°E) (Supplementary Fig. S1a). The average monthly temperature of the study area was 14.1 ± 3.1 °C, with abundant diversity of plant species (Supplementary Fig. S1b). A phylogenetic tree and the corresponding images of the 12 plant species are shown in Fig. 1 and Supplementary Fig. S1c. We collected a total of 144 flower samples, with 12 flower samples collected from 12 distinct individuals of each of the 12 different plant species, which are the most commonly observed wildflowers in this region. The characteristics and species of these plants are summarized in Table 1, based on the available literature [21–23]. Based on their life cycles, the 12 flowering plants were divided into four groups: two annual forbs, four biennial forbs, four perennial forbs, and two perennial trees. The heights of the flowering plants ranged from 5 to 1,200 cm. *V. polita* and *D. indica* were in the group of shorter plants, whereas *P.* × *yedoensis* and *F. koreana* were in the group of taller plants. Although all these plant species engage in insect-mediated pollination, species within the order *Capparales*, such as *B. juncea* and *C. bursa-pastoris*, also undergo self-pollination. Samples were collected from the entire flower, including the receptacle. To prevent cross-contamination, all sampling tools were sterilized with 80% ethanol before and after sample collection.

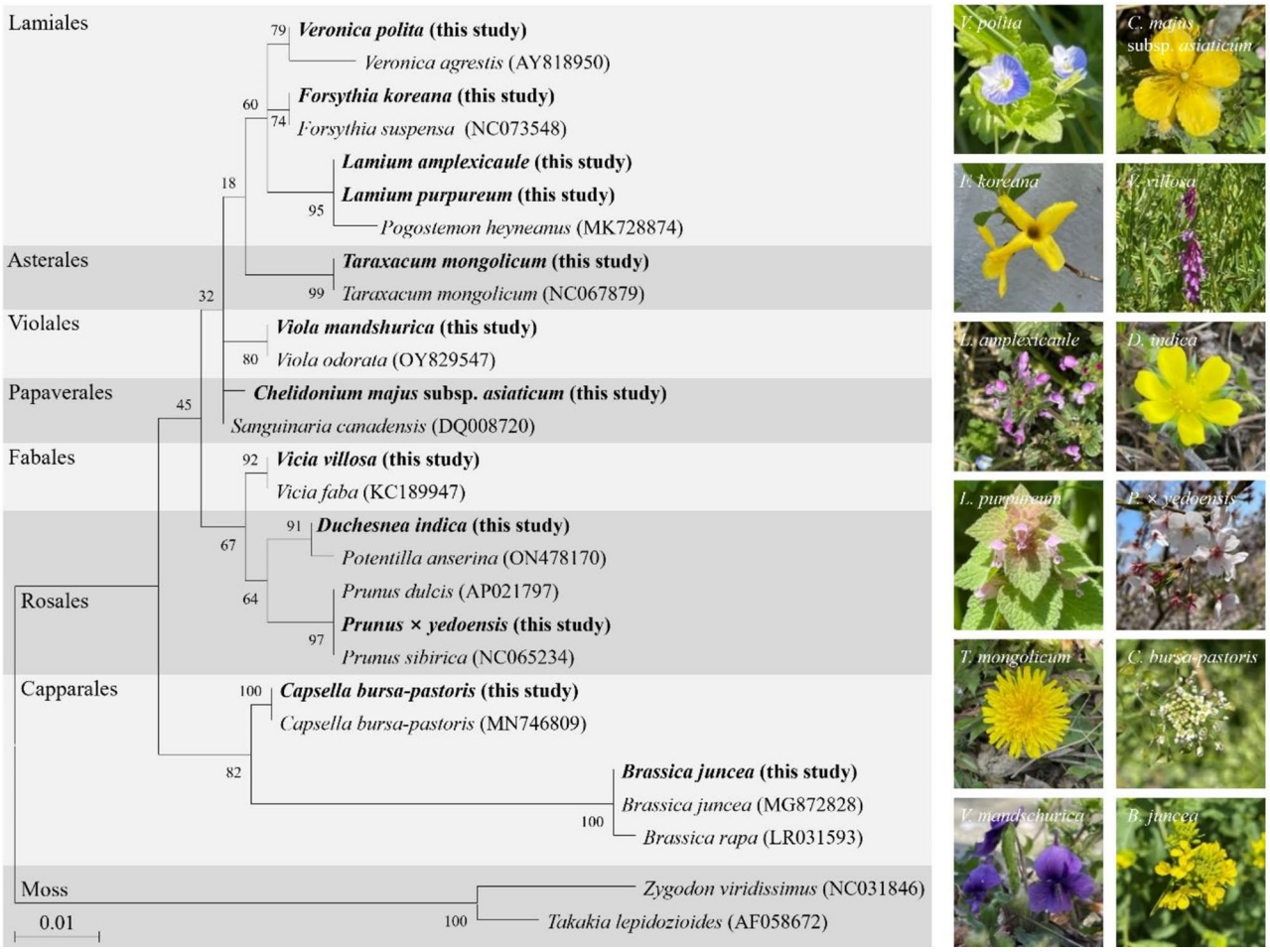


**Fig. 1** Phylogenetic tree of the plant species and representative photographs of flowers used in this study. *Zygodon viridissimu* and *Takakia lepidozioides* were used as outgroups

After collection, the flower samples were immediately frozen at -80℃ to preserve them until DNA extraction in the laboratory.

### DNA extraction, PCR amplification, and sequencing

For DNA extraction, we used the FastDNA™ SPIN Kit for Soil (MP Biomedicals, CA, USA) to isolate genomic DNA. Subsequently, the purity and concentration of DNA were measured using a Nanodrop 2000 UV spectrophotometer (Thermo Fisher Scientific, DE, USA). The extracted DNA was used to construct the Illumina amplicon libraries for bacteria and fungi. The primer set 341 F (5′-TACGGGGGGCAGCAG-3′) and 805R (5′-GGACTACCGGGGTATCT-3′) was used to amplify the V3-V4 region of bacterial 16S rRNA genes [24]. For the fungal internal transcribed spacer 1 (ITS1) region, universal primers ITS1F_KYO1 (5′- CTHGGTCATTTAGAGGAASTAA-3′) and ITS2_KYO2 (5′- TTYRCTRCGTTCTTCATC-3′) were used [25]. Ex Taq™ Hot Start Version (Takara Bio Inc., Otsu, Japan) was used for PCR. To reduce the host DNA amplification, antimitochondrial peptide nucleic acid (mPNA: 5′-GGCAAGTGTTCTTCGGA-3′) and antiplastid peptide nucleic acid (pPNA: 5′-GGCTCAACCCTGGACAG-3′) were introduced, each at a final concentration of 0.25 μM [26]. DNA dimers and residues were removed using Agencourt AMPure XP beads (Beckman Coulter, CA, USA) following the manufacturer's guidelines. To quantify the DNA, we used the Quant-iT dsDNA HS Assay Kit (Thermo Fisher Scientific). Sequencing was conducted using the MiSeq Reagent Kit version 3 (Illumina, CA, USA) for long paired-end reads (2 × 300 bp) at Macrogen Corporation (Seoul, South Korea).

### Bioinformatic analysis

The raw reads obtained were processed using the DADA2 Pipeline Tutorial version 1.16 for bacterial 16S rRNA genes (https://benjjneb.github.io/dada2/tutorial.html) and the ITS Pipeline Workflow version 1.8 for fungal ITS genes (https://benjjneb.github.io/dada2/ITS_workflow.html), and amplicon sequence variants (ASVs) were identified [27]. The latest Silva database (release 138.1) was used to assign the sequences of the 16S rRNA genes

**Table 1** Characteristics of twelve different plant species in this study. The characteristics of each plant species were recorded based on general information referenced from the literature

| Scientific name | Common name | Life cycle | Flowering height (cm) | Inflorescence | Color | Symmetry | Flower composition | Number of | | | Flower size (mm) | Fruit type | Pollinators |
|---|---|---|---|---|---|---|---|---|---|---|---|---|---|
| | | | | | | | | Petals | Stamens | Pistils | | | |
| *Veronica polita* Fr. | Grey field-speedwell | Annual/Biennial forb | 5–15 | Raceme | Blue | Compatible | Free | 4 | 2 | 1 | 2–5 | Capsule | Insects |
| *Forsythia koreana* Nakai | Korean goldenbell tree, Gaenari | Perennial tree | 120–300 | Raceme | Yellow | Radial | Fused | 4 | 2 | 1 | 20–30 | Capsule | Insects |
| *Lamium amplexicaule* L. | Common henbit, Great henbit | Annual/Biennial forb | 30–60 | Cyme | Violet | Compatible | Fused | 2 | 4 | 1 | 15–25 | Follicle | Insects |
| *Lamium purpureum* L. | Red dead-nettle, Purple arcangel | Annual forb | 30–75 | Raceme | Violet | Compatible | Fused | 2 | 4 | 1 | 10–20 | Follicle | Insects |
| *Taraxacum mongolicum* Hand-Mazz | Mongolian dandelion | Perennial forb | 30 | Capitulum | Yellow | Radial | Free | 5 | > 10 | 1 | 30–35 | Achene | Insects |
| *Viola mandshurica* Becker | Violet | Perennial forb | 20 | Solitary | Violet | Compatible | Free | 5 | 5 | 1 | 10–20 | Capsule | Insects |
| *Chelidonium majus* L. subsp. *asiaticum* H.Hara | Greater celandine | Perennial forb | 50 | Raceme | Yellow | Radial | Free | 4 | > 10 | 1 | 10–15 | Capsule | Insects |
| *Vicia villosa* Roth | Hairy vetch, Fodder vetch | Annual/Biennial forb | 30–90 | Raceme | Violet | Compatible | Fused | 5 | 10 | 1 | 10–20 | Legumen | Insects |
| *Duchesnea indica* (Andrews) Teschem. | Indian strawberry, Mock strawberry | Perennial forb | 10 | Cyme | Yellow | Radial | Free | 5 | > 10 | > 10 | 10–15 | Achene | Insects |
| *Prunus* × *yedoensis* Matsum. | Korean flowering cherry | Perennial tree | 200–1200 | Umbel | Pink | Radial | Free | 5 | > 10 | 1 | 20–30 | Drupe | Insects |
| *Capsella bursa-pastoris* (L.) Medik. | Shepherd's purse | Annual/Biennial forb | 30 | Raceme | White | Radial | Free | 4 | 6 | 1 | 2–3 | Nut | Self, Insects |
| *Brassica juncea* (L.) Czern. | Brown mustard | Annual/Biennial forb | 80 | Raceme | Yellow | Radial | Free | 4 | 4–6 | 1 | 10–15 | Nut | Self, Insects |

[28]. For fungi, the UNITE general FASTA release for fungi (version 9.0) was applied [29]. After classifying the sequences, ASVs belonging to the mitochondrial, chloroplast, and non-target sequences were removed. Additionally, to eliminate rare taxa, ASVs with fewer than 10 reads across all samples were excluded from the analysis. After trimming, eight *T. mongolicum* and three *V. polita* bacterial samples and four *L. purpureum* fungal samples were excluded from further analysis because of the limited number of total reads (< 100 reads). Consequently, 133 bacterial and 140 fungal samples were analyzed. The raw sequences and metadata were deposited in the Sequence Read Archive of NCBI under the project accession number PRJNA983070 [30]. Using the "rarecurve" function within the "vegan" package, rarefaction curves were generated [31]. Rarefaction curves reached asymptotes at all taxonomic levels, indicating that sequencing saturation was attained (Supplementary Fig. S2). A phylogenetic tree of the plant species was constructed using the neighbor-joining algorithm [32] in MEGA11 [33] based on mitochondrial sequences obtained from the bacterial 16S rRNA genes dataset in this study (Fig. 1 and Supplementary Fig. S1c). The phylogenetic tree revealed that one-third of the plant species (*V. polita*, *F. koreana*, *L. amplexicaule*, and *L. purpureum*) were classified within the *Lamiales* group, whereas the four plant species belonged to a single order (Fig. 1 and Supplementary Fig. S1c). We categorized ASVs into generalists and specialists to explore their niche dynamics within the anthosphere. Since we also aimed to explore how the identified generalists and specialists contribute to the microbial network and to uncover their roles within it, we included only ASVs that appeared in more than half of the samples for a given plant species and represented at least 0.1% of the total microbial community. ASVs present in more than 10 of the 12 plant species surveyed were categorized as generalists. In contrast, those that appeared in only one or two plant species were classified as specialists. The identified generalists and specialists were visualized using the "UpSetR" package in R [34], and their distribution across the floral samples was depicted using a Venn diagram.

#### Network analysis and microbial function prediction

To identify keystone species and discerning conserved or recurrent patterns within the network [17], we used the sparse inverse covariance estimation for ecological association inference (SPIEC-EASI) method to construct a cross-domain interaction network between bacterial and fungal ASVs in the anthosphere [35, 36]. To filter out rare ASVs, we retained those observed in at least three flower samples per plant species, with an average relative abundance exceeding 0.1%. Calculations were performed according to the following settings: (1) thresh = 0.005; (2) lambda.min.ratio = 0.001; (3) nlambda = 100; (4) method = mb. To identify conserved interactions within the anthosphere, we combined 12 individual networks into a single network, referred to as the "recurrent network", following the methodology described in our previous study [37]. Networks were visualized using the open-source tool Cytoscape version 3.8.2 [38]. Network topological features were analyzed using the "NetworkAnalyzer" plugin in Cytoscape and R software package "igraph" [39, 40]. In the recurrent network, module identification was performed using the Louvain algorithm in R (package: igraph) [40, 41]. Modules appearing in at least ten individual networks were defined as "core modules" in this study. To predict the potential functions of the anthosphere, we performed FAPROTAX analysis for bacteria [42] and FUNGuild analysis for fungi using default settings [43].

#### Statistical analysis

Heatmap and dendrogram analyses were performed using the heatmap.3 function in the "stats" package [44]. The relative abundances of the bacterial and fungal ASVs were subjected to arcsine transformation before constructing a heatmap. The dendrogram was calculated using Euclidean distance. Diversity (Shannon index) and richness (Chao1 index) were calculated using the "vegan" package [31, 45, 46]. One-way analysis of variance (ANOVA) was conducted to assess differences in anthosphere diversity among plant species, followed by Scheffe's post hoc test. Non-metric multidimensional scaling (NMDS) was constructed using the "metaMDS" function (using monoMDS engine) in the "vegan" package, based on bacterial and fungal community composition data separately. The 'envfit' function in the 'vegan' package was then utilized to fit the characteristics of each plant species. The response variable for NMDS was microbial composition, while the explanatory variables included the characteristics of each plant species, with only those showing a significance level of $p < 0.05$ being retained and visualized. Various characteristics of the plant species were categorized into ordinal scales for analysis (Supplementary Table S1). For example, flowering height was classified as 1 (< 30 cm), 2 (30–100 cm), and 3 (> 100 cm), and flower size as 1 (< 5 mm), 2 (5–20 mm), 3 (20–30 mm), and 4 (> 30 mm). To confirm differences among the anthosphere groups, permutational multivariate analysis of variance (PERMANOVA) and analysis of similarity (ANOSIM) were performed using the "adonis2" and "anosim" functions, respectively, within the "vegan" package. Both analyses were based on the Bray-Curtis dissimilarity metric, with microbial community composition as the response variable and plant species as the explanatory variable. A total of 999 permutations were used to

assess the statistical significance of group differences and the extent of separation.

## Results

### Bacterial and fungal community composition

The total number of bacterial ASVs distributed in the surveyed anthospheres was 1,192 with 561,701 reads. The dominant bacterial phyla included *Proteobacteria* (76.4 ± 22.23%) and *Firmicutes* (12.3 ± 21.6%). Notably, *Caulobacter* sp. (ASV0001; 8.8 ± 6.9%) and *Ralstonia* sp. (ASV0002; 8.6 ± 7.5%) were the most prevalent genera (Fig. 2a). Specific associations were observed with *Escherichia* sp. (ASV0010) dominating in *L. purpureum*, and *Pantoea* (ASV0020) predominantly in *B. juncea*. Dendrogram analysis showed that microbial community structures were influenced by characteristics of the plant species such as life cycle, grouping similar life forms together, which contrasted the phylogenetic classifications (Fig. 2b, Supplementary Fig. S3).

In total, 1,521 fungal ASVs were classified using a combined total of 3,332,819 reads. *Ascomycota* (88.56 ± 11.42%) and *Basidiomycota* (9.99 ± 11.33%) were the most abundant fungal phyla. Genera like *Epicoccum* sp. (ASV0033), *Cladosporium* sp. (ASV0034), and *Alternaria* sp. (ASV0035) dominated, together comprising more than half of the fungal community structure (Fig. 2a). However, distinct distribution patterns were noted; for instance, presence of *Epicoccum* presence significantly decreased in *T. mongolicum*, *V. mandshurica*, and *D. indica*.

We categorized the ASVs into generalists and specialists (Fig. 3, Supplementary Tables S1 and S2) and identified eight generalists and 64 specialists (Fig. 3a and b). Among the generalists, four were detected in more than 50% of the flower samples collected from each plant species, except for *T. mongolicum*. For example, *Caulobacter* (BASV0001) appeared in all plant species with a high occurrence rate ranging from 75 to 100% in different plant species (Supplementary Table S2), with an average relative abundance of 8.7 ± 7% in total bacterial community. Two generalist bacteria belonging to the *Sphingomonadaceae* family were identified, and the remaining one was classified as *Achromobacter* (Fig. 3c and Supplementary Table S2). Four fungal ASVs, namely *Epicoccum*, *Cladosporium*, and *Alternaria*, were identified as generalist fungi (Fig. 3d and Supplementary Table S3). Notably, *Cladosporium* (FASV0002) was present in all collected flower samples with relative abundances ranging from 4.2 to 55.7%. *Ceratobasidium* (FASV0023) exhibited a high occurrence exclusively in *T. mongolicum*, whereas *Aureobasidium* (FASV0043) and *Periconia* (FASV0048) showed high occurrence rates in *F. koreana*.

### Alpha and beta biodiversities of the anthosphere

The diversity and richness indices of the anthosphere were calculated to identify differences in microbial composition (Fig. 4). Notably, *F. koreana* exhibited the highest bacterial diversity and richness according to the Shannon index (3.2 ± 0.6, ANOVA; $F = 20.05$, $p < 0.001$) and the Chao1 index (63.7 ± 19.4, ANOVA; $F = 16.65$, $p < 0.001$), whereas *C. bursa-pastoris* and *B. juncea*, both belonging to *Capparales*, showed relatively low bacterial diversity and richness (Fig. 4a and b). Regarding fungal diversity, the indices did not vary significantly among anthospheres according to the Shannon index (Fig. 4c and d, ANOVA; $F = 7.40$, $p = 0.001$); however, differences were observed in the richness indices according to the Chao1 index (ANOVA; $F = 17.46$, $p < 0.001$) (Fig. 4d). The average fungal Shannon index was 2.0 ± 0.4, which was lower than the bacterial index (2.4 ± 0.6). *P.* × *yedoensis* and *D. indica*, both of which belong to the order *Rosales*, showed relatively high levels of fungal diversity and richness according to both Shannon and Chao1 indices. Similar to that in bacteria, anthosphere in *F. koreana* showed the highest fungal richness but not fungal diversity according to the Chao1 index.

To investigate the major drivers of the anthosphere, NMDS ordination was performed using the characteristics of plant species (Fig. 5). ANOSIM and PERMANOVA indicated that bacterial and fungal anthospheres differed significantly according to the plant species (bacteria: ANOSIM, $R = 0.39$, $p = 0.001$; PERMANOVA, $R^2 = 0.28$, $F = 4.20$, $p = 0.001$; fungi: ANOSIM, $R = 0.56$, $p = 0.001$; PERMANOVA, $R^2 = 0.31$, $F = 5.21$, $p = 0.001$). The characteristics of 12 different plant species were fitted to the NMDS plots, revealing that more than half of these characteristics significantly influence the bacterial and fungal anthospheres (Supplementary Table S4). For instance, characteristics such as life cycle, flowering height, pollinators, and inflorescences played crucial roles in shaping both communities, whereas attributes such as flower composition did not have a significant influence. The color and symmetry of the flowers influenced the bacterial anthosphere (Fig. 5a), whereas the number of pistils and stamens affected the fungal anthosphere (Fig. 5b and Supplementary Table S4).

### Microbial network, modules, and microbial function prediction

In this study, we investigated the possible interactions between microbes across and within kingdoms by employing the correlation of co-occurrence patterns using network analysis (Fig. 6). The number of nodes and edges of the individual anthospheric networks ranged from 5 to 108 and 3–97, respectively (Fig. 6a; Table 2). The topological properties of the anthospheric network are summarized in Supplementary Table S5. Notably, *F.*

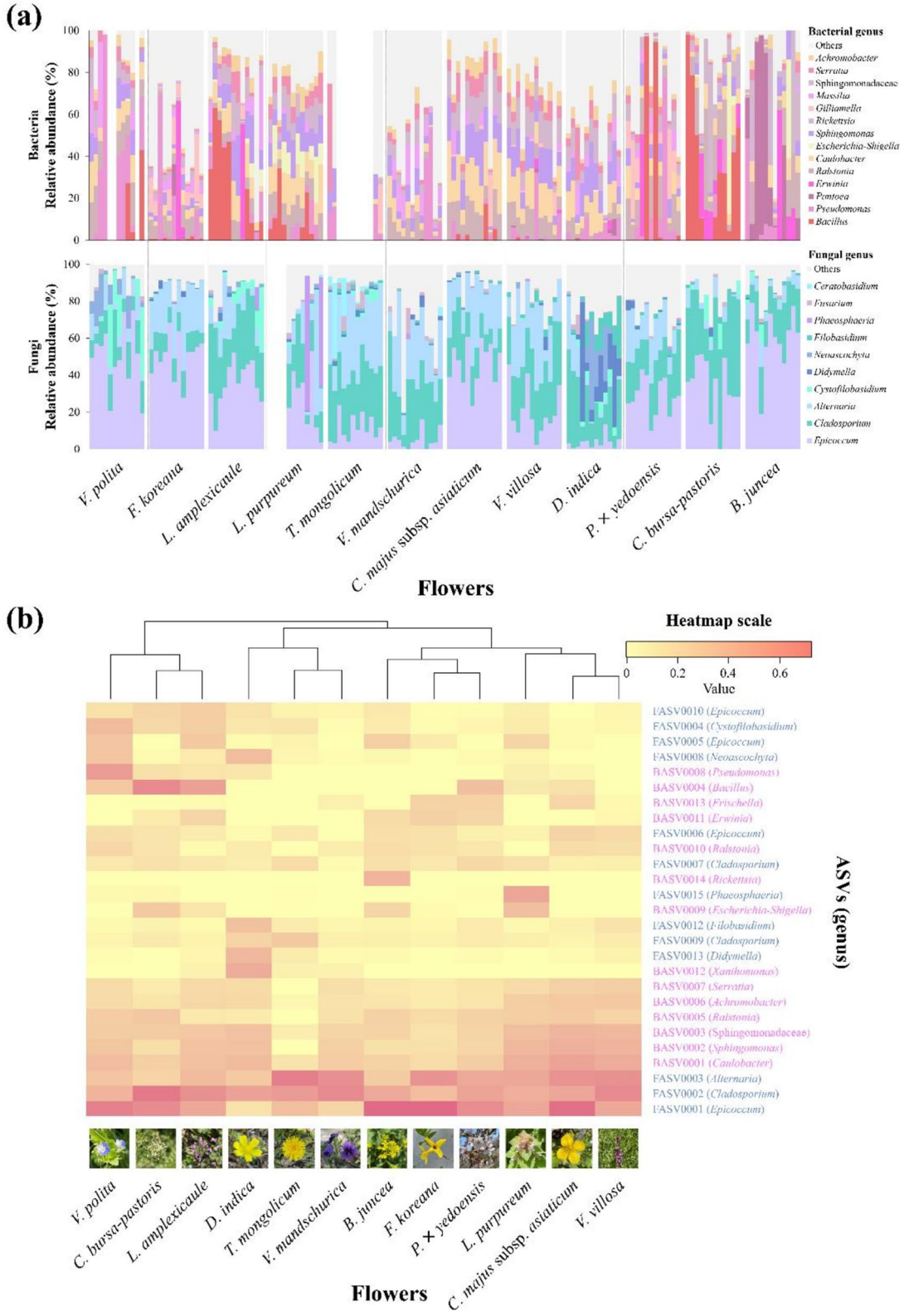


**Fig. 2** The bacterial and fungal community composition. (**a**) Bar plots showing the relative abundances of bacterial (upper panel) and fungal (lower panel) genera in the anthosphere, and (**b**) heatmap showing the major amplicon sequence variants (ASVs) in the anthosphere. 'B' and 'F' in front of ASVs represent bacteria and fungi, respectively

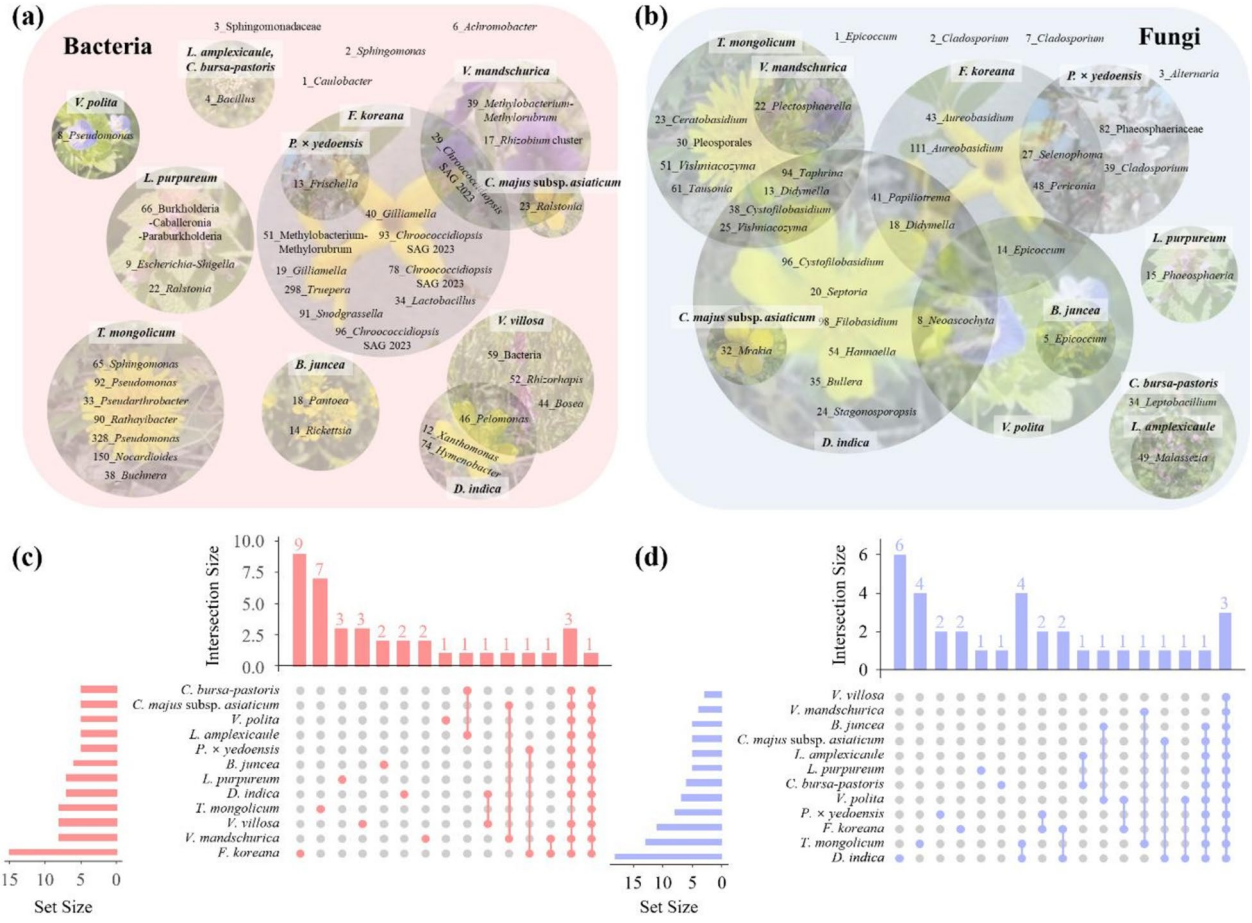


**Fig. 3** Microbial generalists and specialists across different flowers. (**a**) and (**b**) Venn diagrams of the bacterial and fungal generalists and specialists within flowers. The preceding numbers denote the ASV numbers for each kingdom, followed by the genus-level classification. When identification at the genus level was not possible, a higher taxonomic classification is provided. ASVs that are not assigned to any specific group and are enclosed in boxes are represent as generalists. (**c**) and (**d**) UpSet plots of bacteria and fungi showing the intersection sizes of microbial attributes across various flowers, represented by vertical bars. The connected dots below the bars indicate the specific combinations of sample sets where attributes are shared. Horizontal bars show the total attributes present in each set. Vertical bars represent intersection sizes, indicating the number of taxa shared by specific combinations of plant species. Horizontal bars (set sizes) show the total number of taxa found in each individual plant species. The connected dots below the bars indicate the specific combinations of sample sets where attributes are shared

*koreana* showed the most complex network, whereas the networks of *V. polita* and *L. purpureum* displayed only three connections. After combining the individual anthospheric networks into a recurrent network, the modules were calculated to identify any conserved interactions in the anthosphere. Fourteen modules were identified. Conserved recurrent interactions were identified in two core modules (modules 10 and 12; Table 2). Modules 10 and 12 were primarily composed of generalist fungal and bacterial ASVs, respectively (Fig. 6b). Specifically, in module 10, FASV0002 (*Cladosporium*), FASV0003 (*Alternaria*), and FASV0006 (*Epicoccum*) exhibited conserved interactions with FASV0001 (*Epicoccum*). BASV0002 (*Sphingomonas*) interacted at least five times with both BASV0001 (*Caulobacter*) and BASV0003 (*Sphingomonadaceae*) in module 12. On the other hand, several specific modules were identified, including module 5 in *F. koreana* and module 11 in *D. indica*.

FAPROTAX and FUNGuild analyses were performed to infer functional profiles using the identified ASVs (Fig. 7). For bacteria, chemoheterotropic functions showed relatively high abundance throughout the anthosphere, and these functional groups were dominated by various bacteria, such as *Achromobacter*, *Caulobacter*, and *Sphingomonas* (Fig. 7a). Photosynthetic functions driven by *Chroococcidiopsis* were particularly high in *F. koreana* and *V. mandshurica*. Functions related to pathogens or parasites were identified in specific anthospheres, including those of *C. bursa-pastoris* and *B. juncea* (order *Capparales*), which contained ASVs belonging to the genera *Rickettsia* and *Pantoea*. Some species assigned to these genera have been reported to exhibit intracellular parasitic effects and plant pathogenic effects. For

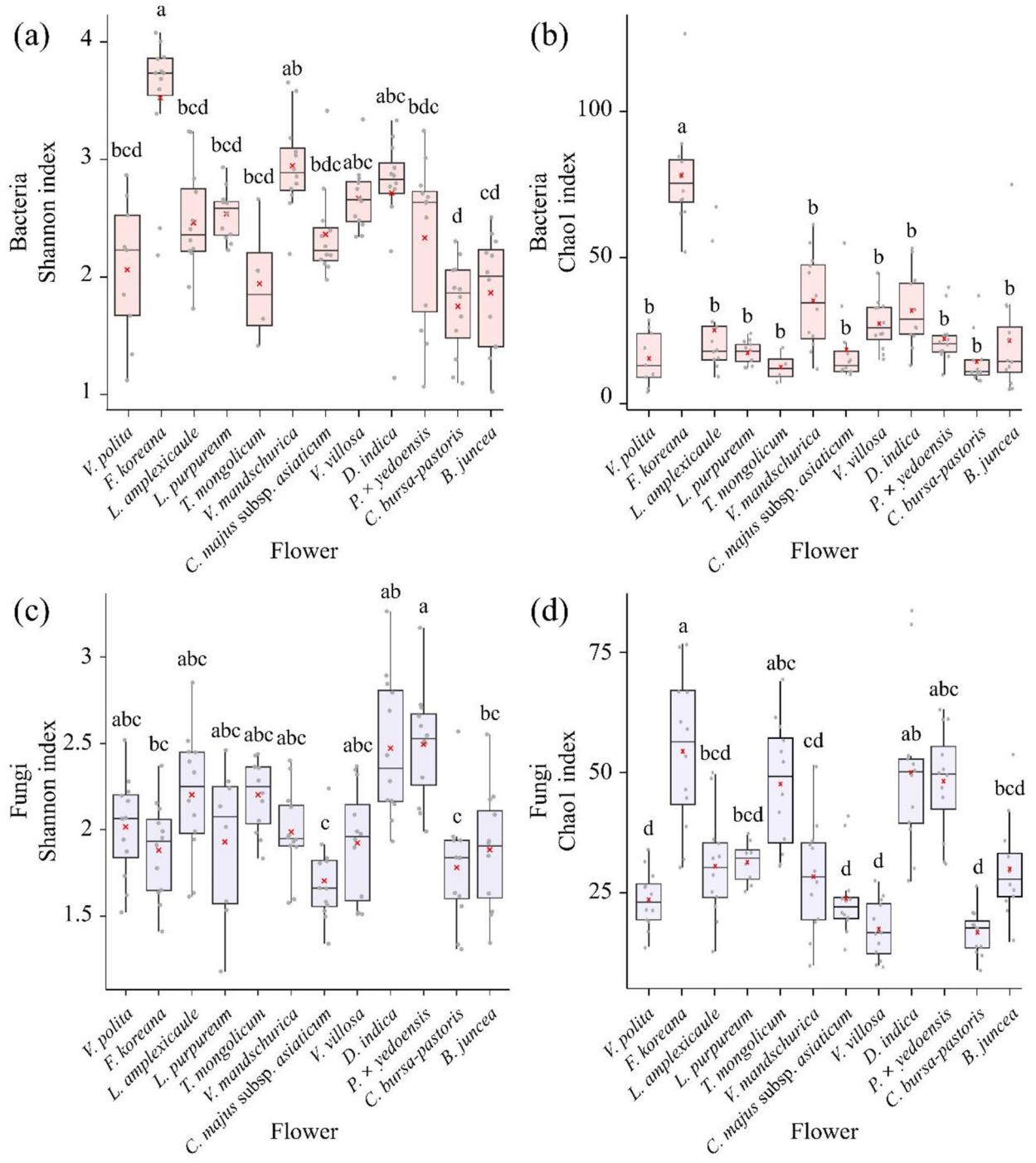


**Fig. 4** Illustration depicting bacterial and fungal biodiversity. (**a**) and (**b**) illustrate the bacterial diversity and richness indices, respectively. Panels (**a**) and (**b**) illustrate the bacterial diversity and richness indices (red boxes), whereas panels (**c**) and (**d**) show the fungal diversity and richness indices (purple boxes). In each panel, the line in the center of the box denotes the median value, whereas the red "X" indicates the mean value. Error bars represent 95% confidence intervals to illustrate variability. Different letters above the boxes indicate significant differences between plant species ($p < 0.05$) based on post-hoc analysis

fungi, functional groups exhibited more complex functional clusters than those of bacteria (Fig. 7b). Functional groups with the highest proportions included pathogens, parasites, and saprotrophs (Supplementary Fig. S4). Notably, the highest proportion of functions belonged to the animal pathogen–plant pathogen–undefined saprotroph group at 35.7 ± 21.3%, followed by those of the endophyte–lichen parasite–plant pathogen–undefined saprotroph group at 17.6 ± 13.9%, accounting for more than half of the total functionality. In contrast,

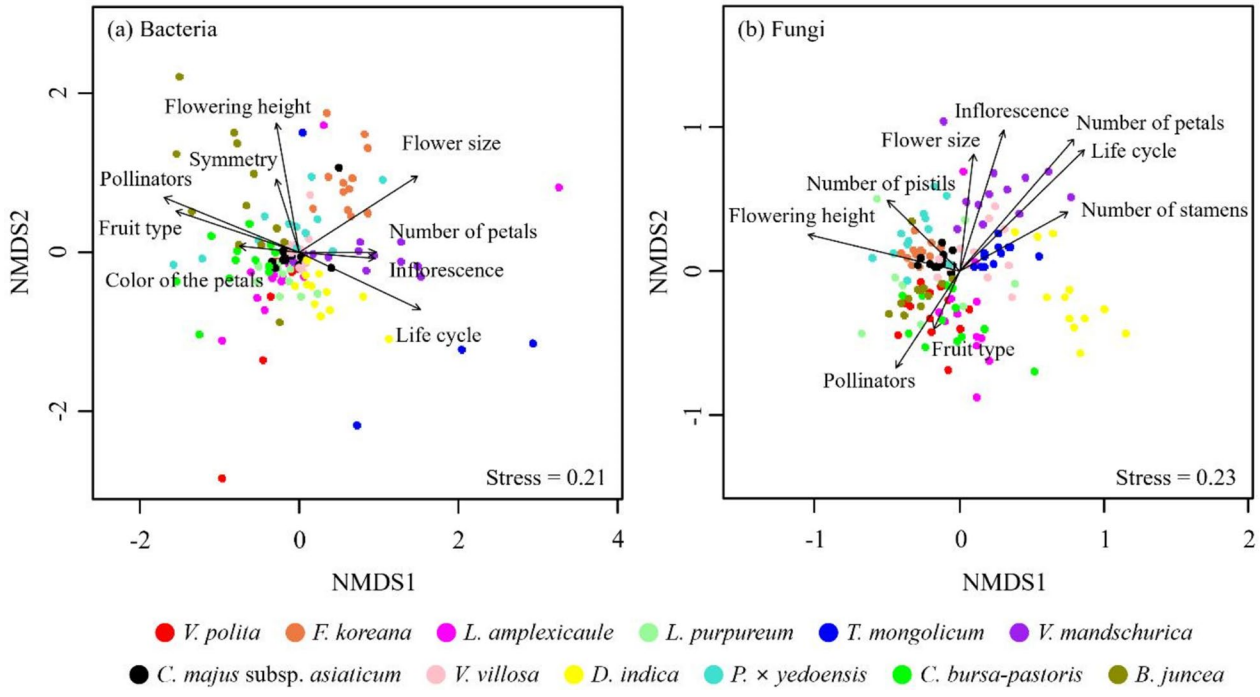


**Fig. 5** Non-metric multidimensional scaling (NMDS) plots of the bacterial and fungal anthosphere and cluster relationships between microbial community structure and characteristics of 12 different plant species. (**a**) NMDS plot for bacterial communities and (**b**) for fungal communities, using Bray-Curtis dissimilarity. (ANOSIM $R = 0.3946$, $p = 0.001$; PERMANOVA $F = 4.2009$, $p = 0.001$, 999 permutations)

endomycorrhizal fungi performed 1.1 ± 5.6% of the total functions in the anthosphere.

## Discussion

The anthosphere is one of the most unique components of the plant holobiont, interacting dynamically with various biotic and abiotic factors, including pollinators [6, 47]. These interactions significantly influence the composition and function of the anthosphere [5]. The anthospheric composition exhibited significant interspecies variation, which is indicative of distinct microbial assemblages associated with different plant species (Fig. 2 and Supplementary Fig. S3). For instance, *Caulobacter*, *Sphingomonas*, and *Achromobacter* were assigned as bacterial generalists and were consistently abundant across all plant species, whereas *Bacillus*, *Escherichia*, *Pantoea*, and *Erwinia* were highly abundant in specific plant. These results are consistent with those of previous studies [48–50]. For example, Rebolleda Gómez and Ashman [49] identified *Acinetobacter*, *Pseudomonas*, *Bacteroides*, *Corynebacterium*, *Erwinia*, and *Lactobacillus* as core bacteria in the anthosphere of *Mimulus guttatus* (yellow monkeyflower). Similarly, *Pseudomonas*, *Pantoea*, and *Sphingomonas* were found to have higher relative abundances in the flowers than in the leaves of *Ranunculus acris* (meadow buttercup) and *Trifolium pratense* (red clover) in grasslands [48]. These results suggest that the primary microbial communities of flowers from different regions were similar and that the intrinsic characteristics of the plant species themselves had a stronger influence than that of the external factors.

The prevalence of specialists, which are dominant in different plant species, emphasizes the intricate interplay between bacterial communities and their host plants, which is likely driven by unique floral traits and microenvironmental conditions [51, 52]. Even within the same environment, microbial community variations were observed in the anthospheres of flower samples collected from the same plant species, highlighting the complex microbial dynamics associated with individual plant species. For instance, *Pantoea* was detected in only one-fourth of the flower samples collected from *B. juncea*, but it dominated these flower samples, reaching a maximum relative abundance of 94.1% (Fig. 2a), which demonstrates the variability of microbial communities within individual plant species. Despite the consistent presence of similar plant species within the same locality, complex interactions between plants and their microbial communities lead to unique microbial assemblages, a phenomenon that contrasts with the relatively homogeneous and simple anthosphere typically observed in cultivated fields [50, 53]. This result indicates that the anthosphere is influenced not only by plant species, but also by randomly occurring external factors, such as visits from pollinators, even for the same plant species inhabiting the same environment.

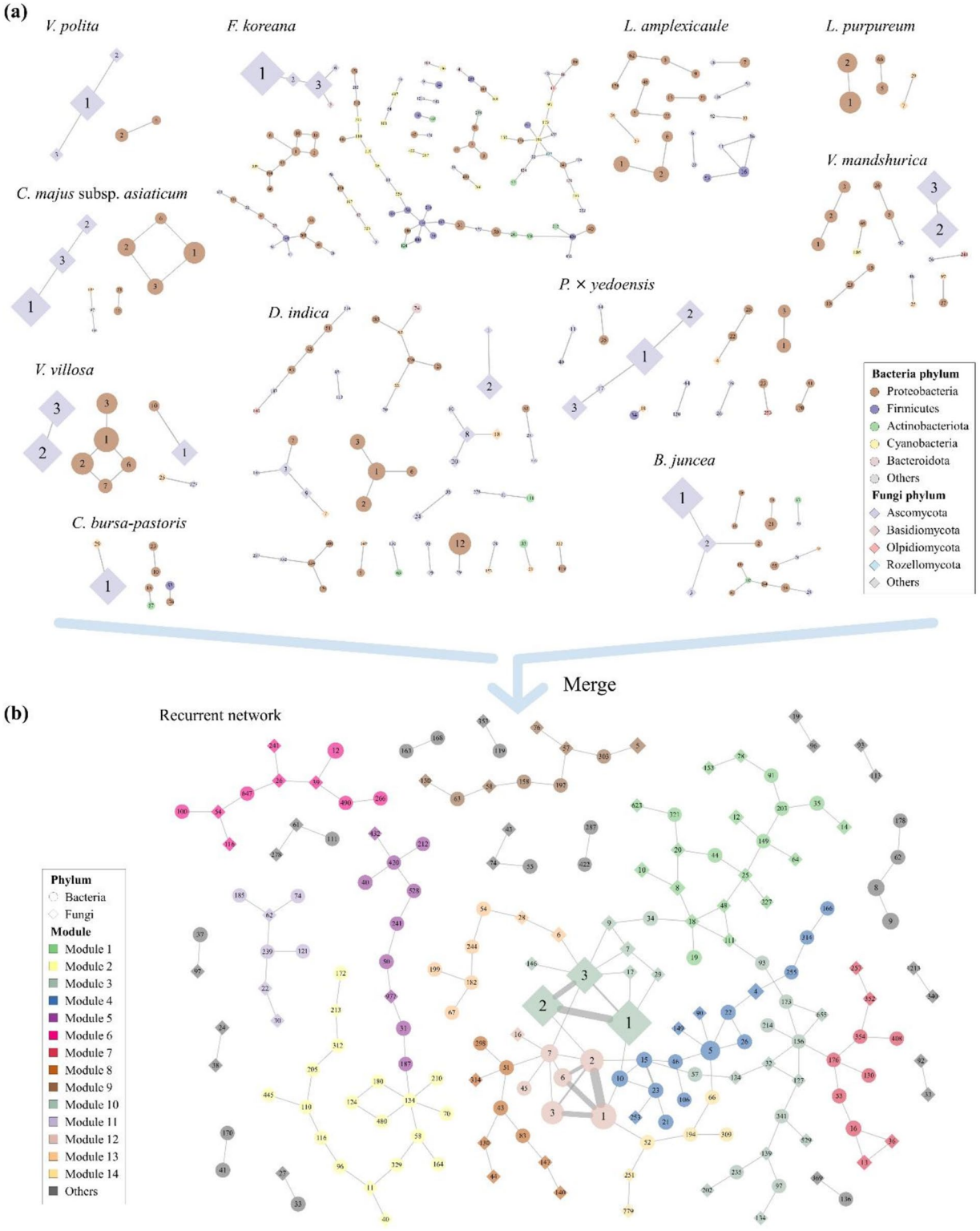


**Fig. 6** Network of microbial interactions between bacterial and fungal anthosphere. Circular and diamond-shaped nodes represent bacteria and fungi, respectively. (**a**) Network of individual anthosphere and (**b**) recurrent network. Node size represents relative abundance of each ASV. The numbers represent each node of the ASV

**Table 2** Frequency of module occurrences derived from network analysis. Nodes that appeared in more than 50% of the members of each module were marked with a circle (○), while those that appeared in 50% or fewer were marked with a triangle (△)

| Flowers | Nodes | Edges | Module | | | | | | | | | | | | | Total |
|---|---|---|---|---|---|---|---|---|---|---|---|---|---|---|---|---|
| | | | 1 | 2 | 3 | 4 | 5 | 6 | 7 | 8 | 9 | 10 | 11 | 12 | 13 | 14 | |
| *V. pollita* | 5 | 3 | | | | | | | | | | △ | | △ | | | 2 |
| *F. koreana* | 108 | 97 | ○ | ○ | ○ | ○ | ○ | ○ | △ | △ | ○ | ○ | | ○ | △ | △ | 13 |
| *L. amplexicaule* | 26 | 17 | | | | ○ | | △ | △ | | △ | | | ○ | △ | | 6 |
| *L. purpureum* | 6 | 3 | | | | △ | | | | | | △ | | △ | | △ | 4 |
| *V. mandschurica* | 19 | 11 | △ | | | ○ | | △ | | | | △ | | △ | | | 5 |
| *C. majus* subsp. *asiaticum* | 12 | 9 | | | △ | △ | | | | | | △ | | △ | | | 4 |
| *V. villosa* | 11 | 8 | △ | | | △ | | | | | | △ | | ○ | | | 4 |
| *D. indica* | 57 | 39 | ○ | | | △ | | △ | △ | ○ | △ | ○ | ○ | ○ | | △ | 10 |
| *P. × yedoensis* | 23 | 13 | △ | △ | | ○ | | △ | | △ | | ○ | | △ | | | 7 |
| *C. bursa-pastoris* | 8 | 4 | | | △ | △ | | | △ | | | △ | | | | | 4 |
| *B. juncea* | 19 | 13 | | | | △ | | | | | △ | △ | | △ | ○ | | 5 |

In this study, the honeybee-related microbes *Achromobacter*, *Frischella*, *Gilliamella*, and *Lactobacillus* were identified in various plant species [54, 55]. Interestingly, among the 12 plant species, the generalist *Achromobacter* demonstrated dominance in 11 plant species, whereas the specialists *Frischella*, *Gilliamella*, and *Lactobacillus* showed a pronounced presence exclusively in *F. koreana*, which exhibited the highest microbial diversity and numerous unique specialists (Figs. 3 and 4 and Supplementary Tables S2 and S3). The specialist genera *Frischella*, *Gilliamella*, and *Lactobacillus* are typically found in the gut of honeybees and play crucial roles in modifying the honey composition and degrading potentially toxic carbohydrates [37, 56]. Although these genera are frequently found in flowers and honeybees, previous studies have shown that they comprise only a minor portion of the honeybee microbiome [5, 57], which is consistent with our findings. In this study, *F. koreana*, a perennial tree intentionally planted for landscaping purposes in South Korea, was located approximately 100 m away from other sampled plant species. This separation in geological location may explain why honeybee-associated microbes were more abundant in *F. koreana* compared to the other 11 plant species. Additionally, previous research has demonstrated that honeybees tend to prefer taller plants, likely due to reduced competition at greater heights, a concept known as the "effective pollination hypothesis" [58, 59].

Previous studies have shown that *F. koreana* contains various phytochemicals, including lignans, flavonoids, diterpenes, and oxygenated monoterpenes [52, 60], while *D. indica* is rich in phytochemicals such as phenolic acids and their derivatives, flavonoids, terpenoids, tannins, lignins, and sterols [51]. Since phytochemicals play key roles in plant defense and ecological interactions and have an impact on shaping microbial communities [61, 62], the unique phytochemical compositions of different plant species may contribute to shaping their specialized microbial communities and driving complex interactions between plant chemistry and microbial ecology in the anthosphere.

Interactions among microbes play crucial roles in shaping microbial communities, as well as the characteristics of plant species and environmental factors [63, 64]. However, our understanding of these interactions in the anthosphere remains limited [17, 20, 65]. Network analysis is widely used and has proven to be highly valuable for studying such biological interactions [19, 66]. Our results revealed that the anthosphere network was relatively simpler than other plant-associated networks, such as the rhizosphere [17]. This phenomenon is likely due to the fact that the flower provides a unique and limited space for microbial communities compared to other plant compartments [67].

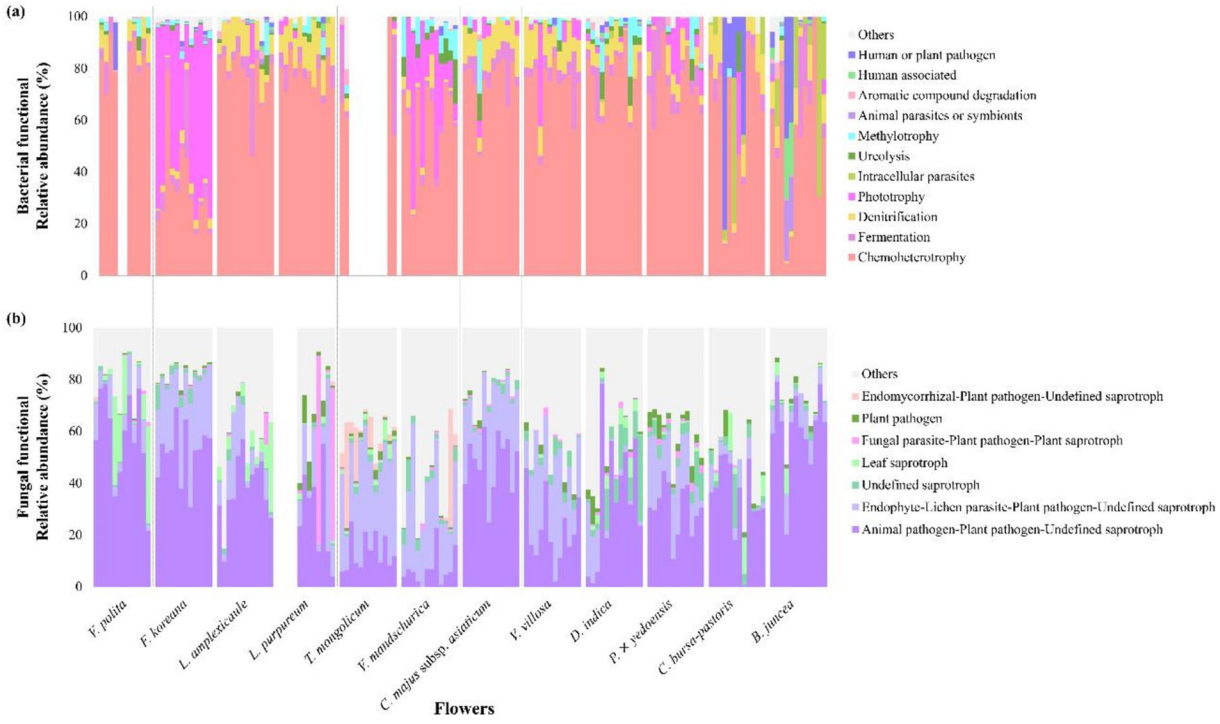


**Fig. 7** FAPROTAX and FUNGuild function prediction of the anthosphere. (**a**) FAPROTAX functional prediction of the anthosphere in 12 different plant species. (**b**) FUNGuild functional prediction of the anthosphere in 12 different plant species

The generalist fungus *Cladosporium* was identified as one of the core microbes and dominated the core module (module 10), which was repeatedly connected with two other generalist fungi, *Epicoccum* and *Alternaria*. Consistent with our results, *Cladosporium* was also identified as a core microbe in the pollen of eight different plant species [20]. Several species belonging to *Cladosporium* have been reported to be isolated from the flowers of various plant species and found in air particles [15, 68]. Since *Cladosporium* produces various antifungal metabolites, such as cladosporin and 5′-hydroxyasperentin [69], these metabolites may serve as a strategy to dominate other fungal groups. Consequently, *Cladosporium*, as a core microbe with unique survival strategies, may serve as a key driver of microbial diversity within the anthosphere through its interactions with other core species.

When specific groups of plant-associated microorganisms, such as those involved in nutrient supply, stress resistance, and bioactive metabolite production, are identified in relatively high proportions, it suggests that these microbes potentially play a vital role in the overall health and metabolic activities of plants [70]. For instance, chemoheterotrophy was the major bacterial function observed in most flowers in this study (Fig. 7a). These functions are primarily carried out by plant growth-promoting rhizobacteria (PGPRs) such as *Caulobacter*, *Pseudomonas*, *Bacillus*, and *Sphingomonas*. Previous studies have indicated that PGPRs attract pollinators by releasing scents from flowers and can delay senescence of flowers [71, 72]. In other studies, bacteria such as *Pseudomonas* and *Bacillus* have been shown to help increase the number of flowers on plants, promote flowering, and extend the flowering period [73, 74]. These findings highlight the crucial role that PGPRs in flowers play in enhancing plant growth and reproductive success. Given their significant functions, PGPRs in the anthosphere could possibly be transmitted to subsequent plant generations through the floral pathway via the stigma of the parent plant, which allows both horizontal and vertical transmission [75], thereby influencing the overall health and productivity of plants across generations. Furthermore, specific anthospheric environments, such as those observed in *C. bursa-pastoris* and *B. juncea* from the *Brassicaceae* family, exhibit the characteristics of intracellular parasites and human or plant pathogens (Fig. 7a). The genera *Bacillus* and *Pantoea* were observed to be specialists in *C. bursa-pastoris* and *B. juncea* (Figs. 2 and 3a; Table 1), respectively. Certain types of bacteria from *Bacillus* and *Pantoea* can cause diseases in plants belonging to the *Brassicaceae* [76, 77]. *C. bursa-pastoris* and *B. juncea* are traditionally consumed as crops in Korea. From our observations at the study site, there were no signs of human presence, such as footprints or other evidence of interaction. This suggests that human handling is unlikely to have contributed directly to the presence of disease-related functions in the plants. However, plants

frequently exposed to human contact may carry such taxa within their holobionts, potentially passing them on through seeds and generations. Additionally, pollinators from nearby cultivated areas could have transferred these taxa during the pollination process.

The relative abundances of fungi varied widely, and accordingly, their functionality also exhibited complex tendencies across plant species (Figs. 2 and 7 and Supplementary Fig. S4). Generally, ectomycorrhizal and saprotrophic fungi dominate other compartments of plants [78, 79]. However, in the present study, functions related to animal or plant pathogens accounted for approximately half of the functional roles in the anthosphere, whereas ectomycorrhizal functions accounted for approximately 1% (Fig. 7b and Supplementary Fig. S4). These results suggest that, unlike in other compartments of the plant, the floral fungal community is influenced by and interacts with various organisms, potentially inducing unique functionalities in the anthosphere. Furthermore, various types of saprotrophic fungi have been identified, which perform over half of the functional roles in the anthosphere. However, undefined saprotrophs were the major group of saprotrophic fungi (Fig. 7b and Supplementary Fig. S4). Previous studies have suggested that floral volatile organic compounds change the function of the anthospheric fungal community in *Osmanthus fragrans* [64]. Further studies are required to determine the specific roles of these undefined saprotrophic fungi in anthosphere.

## Conclusion

This study highlighted the complex and dynamic nature of the wildflower anthosphere. We examined 12 different plant species and uncovered significant variations in microbial communities influenced by unique floral traits and interactions with external factors, such as pollinators. Generalist microbes such as *Caulobacter* and *Sphingomonas* form a foundational core across plant species, whereas *Bacillus* and *Pantoea*, classified as specialists, exhibit plant-specific microbial interactions. The high microbial diversity of *F. koreana*, potentially influenced by honeybee attraction and unique phytochemicals, suggests a role for plant-pollinator interactions in shaping anthospheric communities, although further evidence is needed to fully establish these drivers. Future studies should focus on understanding the specific interactions and roles of anthospheric microbes, particularly the undefined saprotrophic fungi, to deepen our knowledge of anthosphere and their contributions to plant reproductive success and biodiversity.

## Supplementary Information

The online version contains supplementary material available at https://doi.org/10.1186/s40793-025-00666-w.

Supplementary Material 1

**Acknowledgements**
Not applicable.

**Author contributions**
JK: Formal analysis, Visualization, Writing—Original draft preparation; YC: Formal analysis, Visualization, Writing—Original draft preparation; K-HN: Writing—Review and Editing; Funding acquisition, J-WL: Methodology, Investigation, Writing—Review and Editing; J-GK: Writing—Review and Editing; S-JC: Conceptualization, Resources, Writing—Review and Editing, Supervision, Project administration, Funding acquisition. All authors read and approved the final manuscript.

**Funding**
We would like to thank the National Institute of Ecology (NIE) funded by the Ministry of Environment (MOE) of the South Korea (Grant Number: NIE-A-2025-10; NIE-A-2025-04; NIE-A-2025-11).

**Data availability**
The raw sequences, along with the accompanying metadata and detailed parameters used in the pipelines, are accessible in the Sequence Read Archive of NCBI under the project accession numbers PRJNA983070 and published in Data in Brief (Kim et al. 2023).

## Declarations

**Consent for publication**
Not applicable.

**Competing interests**
The authors declare no competing interests.

Received: 4 July 2024 / Accepted: 6 January 2025
Published online: 14 January 2025

**References**

1. Compant S, Samad A, Faist H, et al. A review on the plant microbiome: Ecology, functions, and emerging trends in microbial application. J Adv Res. 2019;19:29–37.
2. Turner TR, James EK, Poole PS. The plant microbiome. Genome Biol. 2013;14:209.
3. Larrouy JL, Dhami MK, Jones EE, et al. Physiological stage drives fungal community dynamics and diversity in *Leptospermum scoparium* (mānuka) flowers. Environ Microbiol. 2023;25:766–71.
4. Aleklett K, Hart M, Shade A. The microbial ecology of flowers: an emerging frontier in phyllosphere research. Botany. 2014;92(4):253-66.
5. McFrederick QS, Thomas JM, Neff JL, et al. Flowers and wild megachilid bees share microbes. Microb Ecol. 2017;73:188–200.
6. Rebolleda-Gómez M, Forrester NJ, Russell AL, et al. Gazing into the anthosphere: considering how microbes influence floral evolution. New Phytol. 2019;224:1012–20.
7. Feltham H, Park K, Minderman J, et al. Experimental evidence that wildflower strips increase pollinator visits to crops. Ecol Evol. 2015;5:3523–30.
8. Aizenberg-Gershtein Y, Izhaki I, Halpern M. Do honeybees shape the bacterial community composition in floral nectar? PLoS ONE. 2013;8:e67556.
9. Qian X, Li X, Li H, et al. Floral fungal-bacterial community structure and co-occurrence patterns in four sympatric island plant species. Fungal Biol. 2021;125:49–61.
10. Rim SO, Roy M, Jeon J, et al. Diversity and communities of fungal endophytes from four *Pinus* species in Korea. Forests. 2021;12:302.
11. Nelson EB. The seed microbiome: origins, interactions, and impacts. Plant Soil. 2018;422:7–34.
12. McArt SH, Koch H, Irwin RE, et al. Arranging the bouquet of disease: Floral traits and the transmission of plant and animal pathogens. Ecol Lett. 2014;17:624–36.

13. Choi HJ, Kim YJ, Park DH. Extended longevity of *Erwinia amylovora* vectored by honeybees under in vitro conditions and its capacity for dissemination. Plant Pathol. 2022;71:762–71.
14. Chen KH, Pannell JR. Disruptive selection via pollinators and seed predators on the height of flowers on a wind-dispersed alpine herb. Am J Bot. 2022;109:1717–29.
15. Sindt C, Besancenot JP, Thibaudon M. Airborne *Cladosporium* fungal spores and climate change in France. Aerobiologia. 2016;32:53–68.
16. Russell KA, McFrederick QS. Floral nectar microbial communities exhibit seasonal shifts associated with extreme heat: potential implications for climate change and plant-pollinator interactions. Front Microbiol. 2022;13:931291.
17. Chun SJ, Cui Y, Yoo SH, et al. Organic connection of holobiont components and the essential roles of core microbes in the holobiont formation of feral *Brassica napus*. Front Microbiol. 2022;13:920759.
18. Ngugi HK, Scherm H. Biology of flower-infecting fungi. Annu Rev Phytopathol. 2006;44:261–82.
19. Barberán A, Bates ST, Casamayor EO et al. Using network analysis to explore co-occurrence patterns in soil microbial communities. ISME J, 2012;6.
20. Manirajan BA, Maisinger C, Ratering S et al. Diversity, specificity, co-occurrence and hub taxa of the bacterial-fungal pollen microbiome. FEMS Microbiol Ecol 2018;94.
21. Missouri Botanical Garden. Missouri botanical garden. Board Trustees; 1893;1893.
22. IPNI, International Plant Names Index. The Royal Botanic Gardens, Kew, Harvard University Herbaria & Libraries and Australian National Herbarium. 2024. http://www.ipni.org. Retrieved 07 June 2024.
23. POWO, Plants of the World Online. Royal Botanic Gardens and Kew. 2024. https://powo.science.kew.org. Retrieved 28 October 2024.
24. Mori H, Maruyama F, Kato H, et al. Design and experimental application of a novel non-degenerate universal primer set that amplifies prokaryotic 16S rRNA genes with a low possibility to amplify eukaryotic rRNA genes. DNA Res. 2014;21:217–27.
25. Toju H, Tanabe AS, Yamamoto S, et al. High-coverage ITS primers for the DNA-based identification of *ascomycetes* and *basidiomycetes* in environmental samples. PLoS ONE. 2012;7:e40863.
26. Fitzpatrick CR, Lu-Irving P, Copeland J, et al. Chloroplast sequence variation and the efficacy of peptide nucleic acids for blocking host amplification in plant microbiome studies. Microbiome. 2018;6:144.
27. Callahan BJ, McMurdie PJ, Rosen MJ, et al. DADA2: high-resolution sample inference from Illumina amplicon data. Nat Methods. 2016;13:581–3.
28. Quast C, Pruesse E, Yilmaz P, et al. The SILVA ribosomal RNA gene database project: improved data processing and web-based tools. Nucleic Acids Res. 2013;41:D590–6.
29. Nilsson RH, Larsson KH, Taylor AFS, et al. The UNITE database for molecular identification of fungi: handling dark taxa and parallel taxonomic classifications. Nucleic Acids Res. 2019;47:D259–64.
30. Kim J, Cui Y, Lee H, et al. Microbiome dataset of bacterial and fungal communities in anthosphere of twelve different wild plants in South Korea. Data Brief. 2023;50:109470.
31. Oksanen J, Simpson GL, Blanchet FG, et al. The vegan package. Community Ecol Package. 2007;10:719.
32. Saitou N, Nei M. The neighbor-joining method: a new method for reconstructing phylogenetic trees. Mol Biol Evol. 1987;4:406–25.
33. Tamura K, Stecher G, Kumar S. MEGA11: molecular evolutionary genetics analysis version 11. Mol Biol Evol. 2021;38:3022–7.
34. Conway JR, Lex A, Gehlenborg N. UpSetR: an R package for the visualization of intersecting sets and their properties. Bioinformatics. 2017;33:2938–40.
35. Chun SJ, Cui Y, Lee CS, et al. Characterization of distinct cyanoHABs-related modules in microbial recurrent association network. Front Microbiol. 2019;10:1637.
36. Kurtz ZD, Müller CL, Miraldi ER, et al. Sparse and compositionally robust inference of microbial ecological networks. PLoS Comput Biol. 2015;11:e1004226.
37. Tipton L, Müller CL, Kurtz ZD, et al. Fungi stabilize connectivity in the lung and skin microbial ecosystems. Microbiome. 2018;6:12.
38. Shannon P, Markiel A, Ozier O, et al. Cytoscape: A software environment for integrated models of biomolecular interaction networks. Genome Res. 2003;13:2498–504.
39. Assenov Y, Ramírez F, Schelhorn S et al. Computing topological parameters of biological networks. Bioinformatics, 2008;24(2):282-4.
40. Csardi G, Nepusz T. The igraph software. Complex Syst. 2006;1695:1–9.
41. Blondel VD, Guillaume JL, Lambiotte R et al. Fast unfolding of communities in large networks. J Stat Mech : Theory Exp, 2008;2008(10):P10008.
42. Louca S, Parfrey LW, Doebeli M. Decoupling function and taxonomy in the global ocean microbiome. Science. 2016;353:1272–7.
43. Nguyen NH, Song Z, Bates ST, et al. FUNGuild: an open annotation tool for parsing fungal community datasets by ecological guild. Fungal Ecol. 2016;20:241–8.
44. Warnes MGR, Bolker B, Bonebakker L et al. Package 'gplots'. Var R Program Tools Plotting data. 2016:112-9.
45. Chao A. Nonparametric estimation of the number of classes in a population. Scand J Stat. 1984;11:265–70.
46. Shannon CE. A mathematical theory of communication. Bell Syst Tech J. 1948;27:379–423.
47. Vannette RL. The floral microbiome: plant, pollinator, and microbial perspectives. Annu Rev Ecol Evol Syst. 2020;51:363–86.
48. Gaube P, Junker RR, Keller A. Changes amid constancy: Flower and leaf microbiomes along land use gradients and between bioregions. Basic Appl Ecol. 2021;50:1–15.
49. Rebolleda Gómez M, Ashman TL. Floral organs act as environmental filters and interact with pollinators to structure the yellow monkeyflower (*Mimulus guttatus*) floral microbiome. Mol Ecol. 2019;28:5155–71.
50. Wei N, Ashman TL. The effects of host species and sexual dimorphism differ among root, leaf and flower microbiomes of wild strawberries in situ. Sci Rep. 2018;8:5195.
51. Fan M, Zhu M, Chen G, et al. *Duchesnea* ganus: A comprehensive review of its phytochemistry, bioactivity, and pharmacology. Phytochem Rev. 2023;22:1585–609.
52. Yang XN, Khan I, Kang SC. Chemical composition, mechanism of antibacterial action and antioxidant activity of leaf essential oil of *Forsythia Koreana* deciduous shrub. Asian Pac J Trop Med. 2015;8:694–700.
53. Manawasinghe IS, Li X, Zhang W et al. Morphological and phylogenetic characterisation of endophytic fungi associated with the grapevine flowers in China. Phytotaxa 2020;455(2):95-118.
54. Powell E, Ratnayeke N, Moran NA. Strain diversity and host specificity in a specialized gut symbiont of honeybees and bumblebees. Mol Ecol. 2016;25:4461–71.
55. Zhang Z, Mu X, Cao Q, et al. Honeybee gut *Lactobacillus* modulates host learning and memory behaviors via regulating tryptophan metabolism. Nat Commun. 2022;13:2037.
56. Zheng H, Nishida A, Kwong WK, et al. Metabolism of toxic sugars by strains of the bee gut symbiont *Gilliamella Apicola*. mBio. 2016;7:e01326–216.
57. Moran NA, Hansen AK, Powell JE, et al. Distinctive gut microbiota of honey bees assessed using deep sampling from individual worker bees. PLoS ONE. 2012;7:e36393.
58. Donnelly SE, Lortie CJ, Aarssen LW. Pollination in *Verbascum thapsus* (*Scrophulariaceae*): the advantage of being tall. Am J Bot. 1998;85:1618–25.
59. Zu P, Schiestl FP. The effects of becoming taller: direct and pleiotropic effects of artificial selection on plant height in *Brassica rapa*. Plant J. 2017;89:1009–19.
60. Lee JJ, Kim KH, Kim EJ, et al. Anti-inflammatory activity of the decoction of *Forsythia suspensa* (Thunb.) Vahl is related to Nrf2 and A20. J Ethnopharmacol. 2018;227:97–104.
61. Macias FA, Galindo JL, Galindo JC. Evolution and current status of ecological phytochemistry. Phytochemistry. 2007;68:2917–36.
62. Harper AD, Stalnaker SH, Wells L, Darvill A, Thornburg R, York WS. Interaction of Nectarin 4 with a fungal protein triggers a microbial surveillance and defense mechanism in nectar. Phytochemistry. 2010;71:1963–9.
63. Hassani MA, Durán P, Hacquard S. Microbial interactions within the plant holobiont. Microbiome. 2018;6:58.
64. Shi T, Shi M, Ye Y, et al. Floral volatile organic compounds change the composition and function of the endophytic fungal community in the flowers of *Osmanthus fragrans*. Int J Mol Sci. 2024;25:857.
65. Wei G, Ning K, Zhang G, et al. Compartment niche shapes the assembly and network of *Cannabis sativa*-associated microbiome. Front Microbiol. 2021;12:714993.
66. Deng Y, Jiang YH, Yang Y, et al. Molecular ecological network analyses. BMC Bioinformatics. 2012;13:113.
67. Russell AL, Ashman TL. Associative learning of flowers by generalist bumble bees can be mediated by microbes on the petals. Behav Ecol. 2019;30:746–55.
68. Prasannath K, Shivas RG, Galea VJ, et al. Novel *Botrytis* and *Cladosporium* species associated with flower diseases of macadamia in Australia. J Fungi. 2021;7:898.
69. Scott PM, Van Walbeek W, MacLean WM. Cladosporin, a new antifungal metabolite from *Cladosporium cladosporioides*. J Antibiot. 1971;24:747–55.

70. Berg G, Köberl M, Rybakova D et al. Plant microbial diversity is suggested as the key to future biocontrol and health trends. FEMS Microbiol Ecol 2017;93(5);fix050.
71. Magalhães DM, Lourenção AL, Bento JMS. Beneath the blooms: unearthing the effect of rhizospheric bacteria on floral signals and pollinator preferences. Plant Cell Environ. 2024;47:782–98.
72. Nayani S, Mayak S, Glick BR. Effect of plant growth-promoting rhizobacteria on senescence of flower petals. Indian J Exp Biol. 1998;36:836–39.
73. Karakurt H, Aslantaş R. Effects of some plant growth promoting rhizobacteria (PGPR) strains on plant growth and leaf nutrient content of apple. J Fruit Ornam Plant Res. 2010;18:101–10.
74. Kumari A, Goyal RK, Choudhary M, et al. Effects of some plant growth promoting rhizobacteria (PGPR) strains on growth and flowering of chrysanthemum. J Crop Weed. 2016;12:7–15.
75. Yaghoubi K, Mohammad S et al. Genetic and ecological inheritance of plant growth-promoting rhizobacteria. Plant Soil. 2024:1–19.
76. Danielsson J, Oleg R et al. Protection of oilseed rape (*Brassica napus*) toward fungal pathogens by strains of plant-associated *Bacillus amyloliquefaciens*. Microbial ecology. 2007;54:134–40.
77. Guo M, Liu Y, Liu SN, et al. First report of bacterial soft rot caused by *Pantoea agglomerans* on Chinese cabbage in China. Plant Dis. 2020;104:277.
78. Deng Q, Wu Y, Zhao X, et al. Influence of different irrigation methods on the alfalfa rhizosphere soil fungal communities in an arid region. PLoS ONE. 2022;17:e0268175.
79. Liang S, Arraiano-Castilho R, Neuenkamp L, et al. Rhizosphere fungal community assembly varied across functional guilds in a temperate forest. Ecol Process. 2023;12:6.

## Publisher's note